AGU PUBLICATIONS

JGR

Journal of Geophysical Research: Space Physics

RESEARCH ARTICLE
10.1002/2015JA021878

Special Section:
Inner Magnetosphere Coupling: Recent Advances

# New global loss model of energetic and relativistic electrons based on Van Allen Probes measurements

Ksenia Orlova[1], Yuri Shprits[2,3], and Maria Spasojevic[4]

[1]Space Center for Research, Education and Innovation, Skolkovo Institute of Science and Technology, Moscow, Russia, [2]Department of Earth, Planetary, and Space Sciences, University of California, Los Angeles, California, USA, [3]Department of Earth, Atmospheric and Planetary Sciences, Massachusetts Institute of Technology, Cambridge, Massachusetts, USA, [4]Department of Electrical Engineering, Stanford University, Stanford, California, USA

**Key Points:**
- Electron lifetime model, 1 keV to 10 MeV for L = 1.5 to 5.5, based on Van Allen Probes hiss statistics
- Comparison with previous lifetimes model developed from CRRES data
- Explore sensitivity of loss to assumed wave intensity and spectral distribution

**Correspondence to:**
M. Spasojevic,
mariaspasojevic@stanford.edu

**Citation:**
Orlova, K., Y. Shprits, and M. Spasojevic (2016), New global loss model of energetic and relativistic electrons based on Van Allen Probes measurements, *J. Geophys. Res. Space Physics*, *121*, 1308–1314, doi:10.1002/2015JA021878.

Received 3 SEP 2015
Accepted 19 JAN 2016
Accepted article online 22 JAN 2016
Published online 19 FEB 2016



**Abstract** The Electric and Magnetic Field Instrument Suite and Integrated Science (EMFISIS) instrument on the Van Allen Probes provides a vast quantity of fully resolved wave measurements below $L = 5.5$, a critical region for radiation belt acceleration and loss. EMFISIS data show that plasmaspheric hiss waves can be observed at frequencies as low as 20 Hz and provide three-component magnetic field measurements that can be directly used for electron scattering calculations. Updated models of hiss properties based on statistical analysis of Van Allen Probes data were recently developed. We use these new models to compute and parameterize the lifetime of electrons as a function of kinetic energy, *L* shell, *Kp* index, and magnetic local time. We present a detailed analysis of the electron lifetime sensitivity to the model of the wave intensity and spectral distribution. We also compare the results with previous models of electron loss, which were based on single-component electric field measurements from the sweep frequency receiver on board the CRRES satellite.

## 1. Introduction

Observations from the OGO satellite series first showed persistent incoherent whistler mode emissions in the ELF/VLF frequency range in the near-Earth space environment, and these waves are commonly referred to as plasmaspheric hiss [e.g., *Russell et al*., 1969; *Thorne et al*., 1973]. The origin of plasmaspheric hiss remains an active topic of scientific research [e.g., *Thorne et al*., 1979; *Sonwalkar and Inan*, 1989; *Meredith et al*., 2006a; *Bortnik et al*., 2008; *Chen et al*., 2012a, 2012b, 2012c]. Quantification of the quasi-linear scattering rates [e.g., *Kennel and Engelmann*, 1966; *Lerche*, 1968] by these waves [*Lyons et al*., 1972] showed that hiss waves play a dominant role for the loss of the radiation belt electrons and are responsible for the formation of the slot region [*Lyons and Thorne*, 1973]. Scattering by hiss waves also affects ring current electrons, and *Chen and Schulz* [2001a, 2001b] created the first models, which at higher *L* shells had a smooth transition to the strong diffusion lifetime. *Shprits et al*. [2005, 2006a] provided a parametrization of electron loss in the radiation belts based on the visual comparison of radial diffusion modeling with observations. To reproduce observations, *Shprits et al*. [2005, 2006] used parameterizations of lifetime of $\tau = 3/Kp$ for simulations with a constant outer boundary and $\tau = 5/Kp$ for a variable outer boundary. The electron lifetimes inside the plasmasphere due to hiss waves were modeled with a constant decay rate of 10 days. Physics-based modeling of electron lifetimes requires detailed knowledge of how wave amplitude depends on geomagnetic activity, radial distance, magnetic latitude and magnetic local time (MLT), and also detailed knowledge of the wave spectral and wave normal distributions.

Statistical analysis of hiss wave distributions have shown that waves are present for a broad range of MLT but are more intense on the dayside, extend to high latitudes above 30°, and that wave amplitudes are activity dependent [e.g., *Meredith et al*., 2004; *Golden et al*., 2012; *Agapitov et al*., 2013; *Li et al*., 2015]. *Orlova et al*. [2014] provided empirical parameterizations of wave activity and also derived a parametric model of electron lifetimes based on Sweep Frequency Receiver measurements from the CRRES mission. The analytical model of electron lifetimes from *Orlova et al*. [2014] can be incorporated into convective simulations and particle tracing codes and can be also used to estimate the precipitating flux of kiloelectron volt electrons that control ionospheric conductivity. A number of studies showed that conversion of power from electric wave measurements to magnetic field quantities, as is done with the CRRES data, may be rather inaccurate due to uncertainties in wave normal distributions of waves [e.g., *Ni et al*., 2011; *Spasojevic et al*., 2015]. Van Allen Probes observations also revealed the presence of non-Gaussian spectral distribution and low-frequency waves at

frequencies below 100 Hz that were not accounted for by the previously developed models [*Li et al*., 2013, 2015]. *Spasojevic et al*. [2015] recently presented an improved empirical model of plasmaspheric hiss intensity obtained using statistical analysis of Van Allen Probes measurements for 2 years. By performing statistics over the large data set, *Spasojevic et al*. [2015] parameterized the hiss intensity as a continuous function of geomagnetic activity including storm time conditions.

To incorporate this knowledge gained from the Van Allen Probes mission, new parameterizations of electron loss should be developed and compared to the previously developed model to provide a framework for analysis of previous results and to understand how models are improved by introducing the newly developed parameterizations. In this study, we present a new loss model based on Van Allen Probes observations that is capable of accurately predicting loss during disturbed geomagnetic conditions. Next, we compare the newly developed model with a previously developed model based on CRRES wave data. We also examine the sensitivity of the scattering rates to the assumed spectral distribution and the assumed distribution of wave intensity.

## 2. Electron Lifetimes

### 2.1. Calculation and Parameterization of Lifetimes

Loss of particles due to pitch angle diffusion can be presented as a superposition of exponentially decaying normal modes [*Schulz and Boucher*, 1982]. As the lowest normal mode decays slower than other modes, it is customarily assumed that the particles decay to some equilibrium (lowest normal mode) quickly, then distribution continues to decay with a rate constant at all pitch angles [e.g., *Schulz and Lanzerotti*, 1974; *Shprits et al*., 2008]. If scattering rates as a function of pitch angle are relatively monotonic or at least do not show significant minimums of 1 order of magnitude or more, the loss time can be estimated by taking an inverse of the pitch angle scattering rates near the edge of the loss cone [*Lichtenberg and Lieberman*, 1983; *Shprits et al*., 2006b]. If the pitch angle diffusion coefficients have a deep local minimum for a wide range of pitch angles, they can create bottleneck and slow down the overall rate of pitch angle scattering. In this study we use the expression of *Albert and Shprits* [2009] that utilizes pitch angle diffusion rates at all values of equatorial pitch angle to calculate electron lifetime, $\tau$:

$$\tau = \int_{\alpha_{lc}}^{\pi/2} d\alpha_{eq} \left(2 \ < D_{\alpha\alpha} > \ \tan\left(\alpha_{eq}\right)\right)^{-1}, \tag{1}$$

where $\alpha_{eq}$ is the equatorial pitch angle and $\alpha_{lc}$ is the equatorial loss cone angle. $<D_{\alpha\alpha}>$ is the bounce-averaged pitch angle diffusion coefficient computed in the dipole field using an approach of *Glauert and Horne* [2005] and *Albert* [2005]. For the hiss intensity below the magnetic latitude of 20°, we took the simplified model of *Spasojevic et al*. [2015] obtained using Van Allen Probes measurements and used $< B_w^2 > = 10^{0.05894L^3 - 0.7768L^2 + 3.163L - 1.036}$ (valid for $1.2 \le L \le 6.1$ and latitudes less than 20°) for the averaged MLT = 18.007 and $Kp = 2.683$ values in our computations. Note that we first develop a simple model with just $L$ and electron energy and then later use the results of *Spasojevic et al*. [2015] to extend to other MLT and $Kp$ values. Since *Spasojevic et al*. [2015] showed that hiss wave intensity is almost independent of magnetic latitude, we extended the hiss amplitude model up to 45° following previous studies [e.g., *Agapitov et al*., 2013]. The wave normal angle distribution, plasma density, and number of resonances are the same as in *Orlova et al*. [2014] and are based on *Agapitov et al*. [2013], *Denton et al*. [2004, 2006], and *Mourenas and Ripoll* [2012]. For the hiss spectrum, we used a realistic distribution obtained from the statistical analysis of the Electric and Magnetic Field Instrument Suite and Integrated Science (EMFISIS) measurements on Van Allen Probes by *Li et al*.[2015] ranging between 20 Hz and 4000 Hz. The maximum of spectrum of *Li et al*. [2015] $f_m$ is dependent on $L$, for example, at $L = 2$ $f_m = 82$ Hz and at $L = 5$ $f_m = 142$ Hz. The previous conventional spectral model assumed $f_m = 550$ Hz. Since *Li et al*. [2015] presented the spectral model for discrete $L = 2$, 3, 4, and 5, we considered that it is valid for the range of $L \pm 0.5$. At the junction of spectral models $L = 2.5$, 3.5, and 4.5 we computed the diffusion coefficients for both models and average them.

Figure 1a shows calculated lifetimes $\tau_{av}$ for the averaged MLT and $Kp$ values as a function of electron kinetic energy $E_k$ from 1 keV up to 10 MeV and $L$ shells from 1.5 to 5.5. The dark red color represents the regions with lifetimes larger than 1000 days. Lifetimes tend to decrease with increasing $L$ from 1000 days to the values of several days or even less than a day at $L > 4$ for tens of keV electrons. There is also a strong dependence of

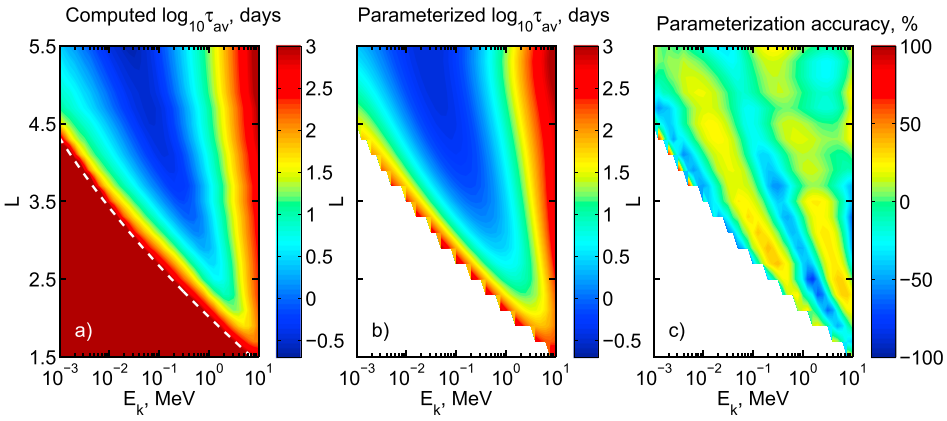


**Figure 1.** (a) Computed and (b) parameterized lifetimes $\log_{10}\tau_{av}$, in days, and (c) parameterization accuracy as a function of electron kinetic energy and $L$ shell. White line in Figure 1a illustrates energies above which parameterization of lifetimes is valid.

lifetimes on energy. At a given $L$, a slice in energy has a local minimum in $\tau_{av}$. With increasing $L$, the value of the minimum lifetime becomes shorter and moves to lower energy. For example, the minimum lifetime at $L = 3.1$ is 1.4 days at $E_k = 630$ keV and at $L = 5.1$ is around 7.5 h at $E_k = 40$ keV. It should be noted that the inner belt lifetimes are larger than a thousand days for almost all the nonrelativistic energies.

Electron lifetimes are parameterized as a function of $L$ and kinetic energy by applying linear regression for values less than 1000 days, which are most physically meaningful:

$$log_{10}\tau_{av}(L,E) = a_1 + a_2L + a_3E + a_4L^2 + a_5LE + a_6E^2 + a_7L^3 + a_8L^2E + a_9LE^2 + a_{10}E^3 + a_{11}L^4 + a_{12}L^3E + a_{13}L^2E^2 + a_{14}LE^3 + a_{15}E^4 + a_{16}LE^4 + a_{17}L^2E^3 + a_{18}L^4E + a_{19}L^5 + a_{20}E^5, \quad (2)$$

where $E = \log_{10}E_k$ for $E_k$ from 1 keV up to 10 MeV taken in MeV units and $L$ is in the range from 1.5 up to 5.5. The parameterization in equation (2) is valid for energies $E \geq f(L)$, where $f(L) = 0.1328\,L^2 - 2.1463\,L + 3.7857$ (above the white line in Figure 1a). Coefficients of parameterization, $a_n$, in equation (2) are presented in Table 1. We illustrate the parameterized lifetimes in Figure 1b where white areas correspond to $E < f(L)$. Figure 1c shows the accuracy of parameterization, which is defined as $\left(\tau^c_{av} - \tau^p_{av}\right)/\tau^c_{av}$ where $\tau^c_{av}$ is the computed lifetime and $\tau^p_{av}$ is the parameterized lifetime. While for most energies and $L$ shells the parameterization error is less than ±25%, the mean value is 17.8%, and the maximum parameterization error reaches 75.7%. Most likely the error of the parameterization is less than uncertainty associated with the assumed plasma and wave models.

**Table 1.** Coefficients for Electron Lifetime Parameterization in Equation (2)

| | Values |
|---|---|
| $a_1$ | 77.323 |
| $a_2$ | −92.641 |
| $a_3$ | −55.754 |
| $a_4$ | 44.497 |
| $a_5$ | 48.981 |
| $a_6$ | 8.9067 |
| $a_7$ | −10.704 |
| $a_8$ | −15.711 |
| $a_9$ | −3.3326 |
| $a_{10}$ | 1.5189 |
| $a_{11}$ | 1.294 |
| $a_{12}$ | 2.2546 |
| $a_{13}$ | 0.31889 |
| $a_{14}$ | −0.85916 |
| $a_{15}$ | −0.22182 |
| $a_{16}$ | 0.034318 |
| $a_{17}$ | 0.097248 |
| $a_{18}$ | −0.12192 |
| $a_{19}$ | −0.062765 |
| $a_{20}$ | 0.0063218 |

Since the simplified model of hiss intensity of *Spasojevic et al.* [2015] has a separate dependence on magnetic local time and geomagnetic activity, for the chosen MLT and *Kp* values lifetimes of electron can be obtained as

$$\tau(L,E,\mathrm{MLT},Kp) = \frac{\tau_{av}(L,E)}{g(\mathrm{MLT})h(Kp)}, \quad (3)$$

where functions $g$(MLT) and $h$(*Kp*) are given in equations (4) and (6) of *Spasojevic et al.* [2015], respectively, and are valid for $1.5 \leq L \leq 5.5$. Note that equation (3) was derived for *Kp* values up to 5.

### 2.2. Comparison of the Global loss Models

There are two differences between the global loss model of *Orlova et al*. [2014] and the new one presented here. To compute the lifetimes, *Orlova et al*. [2014] considered the conventional hiss frequency model based on CRRES data [e.g., *Shprits et al*., 2009; *Thorne et al*., 2013] with the following Gaussian spectrum parameters $f_m = 550$ Hz, $\delta f = 300$ Hz, $f_{lc} = 100$ Hz, and $f_{uc} = 2000$ Hz. For the hiss intensity *Orlova et al*. [2014] developed and used an empirical model based on single-component electric field measurements from the sweep frequency receiver on board the CRRES satellite. For the new loss model presented in section 2.1, we used the hiss intensity model of *Spasojevic et al*. [2015] based on three-component magnetic field measurements of the EMFISIS instrument on Van Allen Probes. We also used a realistic spectrum model based on statistical analysis of Van Allen Probes measurements of *Li et al*. [2015] for which the maximum frequency and the lower and upper cutoffs are less than in the conventional frequency model.

To compare the two loss models, we examine $L$ shells in the range of 3 to 5.5 where both empirical wave models are valid. We focus on the dayside local time sector $6 \leq \mathrm{MLT} \leq 21$ where hiss activity is strongest and performed MLT averaging of the new loss model for the considered sector. Below we denote $\tau_N$ as the new lifetimes presented in section 2.1 and $\tau_O$ the old ones from *Orlova et al*. [2014]. Figures 2a–2f illustrate the lifetimes $\tau_O$ and $\tau_N$, respectively, for various levels of geomagnetic activity $Kp = 0.75$, 3, and 4.5. The dark red color corresponds to lifetimes larger than 1000 days. The difference in loss models $(\tau_N - \tau_O)/\tau_N$ is presented in Figures 2g–2i and is dependent on energy and distance. Areas with deep blue color have a difference less than −400%. For relativistic energies the difference between two loss models is 2.5 times or less (from −40% to 60%). For $E_k < 100$ keV at $L > 4.1$ and for energies of tens and hundreds keV at $L < 4.1$ the old model shows significantly longer lifetimes $5\tau_N < \tau_O$. It should be noted that the old model of *Orlova et al*. [2014] did not match the observed electron decay rates of several days [*Meredith et al*., 2006b; *Benck et al*., 2010] for energies 150–400 keV at $3 < L < 3.6$ where the computed lifetimes reached the values of tens or hundred days. The new model is capable of reproducing the observations at these distances and energies.

### 2.3. Sensitivity of Lifetimes to Hiss Properties

Figure 3 shows how the introduction of more accurate models of hiss waves influence electron lifetimes at $L = 3$ (Figure 3a) and $L = 4$ (Figure 3b) on the dayside (6–21 MLT) for $Kp = 3$. The lifetimes computations using CRRES hiss wave intensity and conventional frequency models [e.g., *Meredith et al*., 2007; *Orlova et al*., 2014] are presented by the solid blue color in Figure 3. The dashed black line shows the results of the calculations using the same amplitude model but with the realistic frequency based on Van Allen Probes data, as discussed above. Electron lifetimes computed using the new hiss intensity model of *Spasojevic et al*. [2015] based on Van Allen Probes measurements and the conventional frequency model are shown by the dashed green color. Finally, the solid red color corresponds to calculations of the lifetimes using the Van Allen Probes intensity model and Van Allen Probes frequency model.

The introduction of the new spectral distribution of waves not only extends the range of hiss frequencies but also redistributes the power. Lifetimes computed using the realistic spectrum are shorter than those calculated for conventional frequency model (compare dashed black curve to blue curve, dashed green curve to red curve). While at multi-MeV energies the difference is no more than 2.5 times, at lower energies the lifetimes can differ by several orders of magnitude.

Next, we consider calculations using the same frequency model but with different intensity models (compare blue curve to dashed green curve, dashed black curve to red curve). The use of the Van Allen Probes $< B_w^2 >$ model increases the lifetimes of electrons at keV and tens of keV energies and at relativistic energies $E_k > 1$ MeV by a factor up to 3.5. For the middle energies of hundreds of keV lifetimes computed for CRRES intensity model are similar to those calculated for Van Allen Probes $< B_w^2 >$ model.

Lastly, the total effects of using the new models of hiss intensity and frequency distribution are not as straightforward as from separately changing hiss frequency and amplitude and are dependent on both energy and distance (compare blue and red curves). At some energies, for example, 20 keV–1 MeV at $L = 3$ and 2–200 keV at $L = 4$, the total difference in lifetimes is mainly caused by the change of frequency model. At multi-MeV energies the effects of changing each property work in the opposite directions and the lifetimes computed for the CRRES intensity model and conventional frequency model are shorter than those computed for the Van Allen Probes $< B_w^2 >$ model and Van Allen Probes frequency model by less than a factor of 2.5.

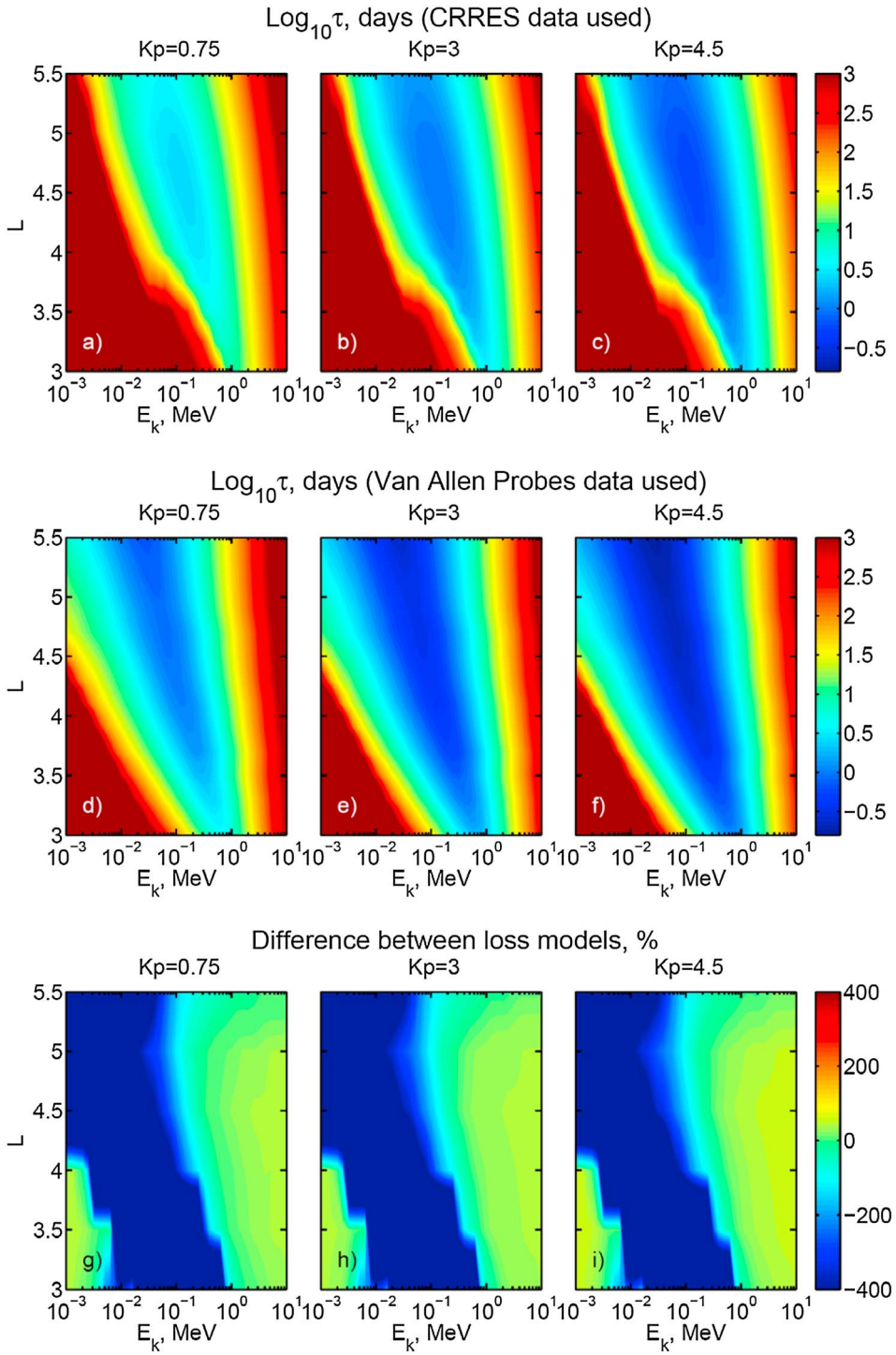


**Figure 2.** Comparison of MLT-averaged electron lifetimes on the dayside (MLT = 6–21) computed (a–c) using CRRES amplitude model and conventional frequency model [*Orlova et al.*, 2014] and (d–f) using Van Allen Probes intensity model and Van Allen Probes frequency model as a function of *L* shell and electron kinetic energy for various *Kp* indices. (g–i) The percent difference between the two models.

## 3. Summary

We present the updated global electron loss model based on the recent models from Van Allen Probes measurements of hiss wave intensity of *Spasojevic et al.* [2015] and realistic spectral distributions of *Li et al.* [2015]. The loss model is strongly dependent on electron kinetic energy and *L* shell and lifetimes can be less than a

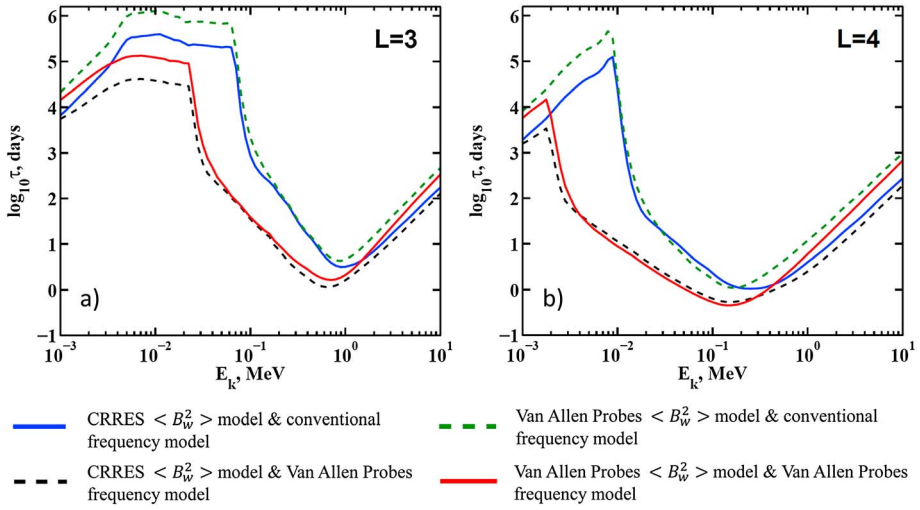


**Figure 3.** Sensitivity of MLT-averaged electron lifetimes on the dayside (MLT = 6–21) to hiss amplitude and frequency models at (a) $L = 3$ and (b) $L = 4$ as a function of electron kinetic energy for $Kp = 3$.

day at large distances for tens of keV electrons. The computed lifetimes are parameterized as a function of $L$ in the range of 1.5 to 5.5 and kinetic energy in the range of $E_k = 1$ keV to 10 MeV and can differ up to 4 times from the calculated losses. The dependence of lifetimes on geomagnetic activity (for $Kp \leq 5$) and MLT (0–24) can be taken from the simplified model of hiss intensity of *Spasojevic et al*. [2015], and thus, the new loss model can be widely implemented in convection and particle tracing codes.

We compared the newly obtained global loss model with the previous lifetimes model of *Orlova et al*. [2014], which was based on the CRRES hiss intensity model and conventional frequency distribution. It was shown that the difference between two loss models at nonrelativistic energies is several orders of magnitude. Note that the new loss model also covers the slot region and inner belt, which was not available from *Orlova et al*. [2014].

We investigated the sensitivity of electron lifetimes to the change of hiss properties such as wave intensity and frequency distribution. We computed the lifetimes for two hiss intensity models, from CRRES [*Orlova et al*., 2014] and Van Allen Probes [*Spasojevic et al*., 2015], and two frequency models, one conventional and one obtained from Van Allen Probes measurements [*Li et al*., 2015]. The effect of more accurately modeling hiss properties can be small, on the order of several times at relativistic energies, or can provide a difference of several orders of magnitude to the resulting lifetimes at lower energies. Thus, the wave parameters used in calculations of electron lifetimes play an important role, and future research is needed to explore the extension of hiss intensity to high latitudes as well as obtain global models of wave normal angles for a wide range of distances.

**Acknowledgments**
This research was supported by NSF AGS120374; NASA NN15AJ94G, NNX13AE34G, and NNX10AK99G; and UC Lab Fees Research Program grant 12-LR-235337. The work of M. Spasojevic was supported by NASA awards NNX14AC04G and NNX15AI94G. The authors thank the EMFISIS team for the Van Allen Probes data, which were accessed through the EMFISIS website hosted at the University of Iowa. All data sets used in this study can be accessed by contacting the first author.

## References

Agapitov, O., A. Artemyev, V. Krasnoselskikh, Y. V. Khotyaintsev, D. Mourenas, H. Breuillard, M. Balikhin, and G. Rolland (2013), Statistics of whistler-mode waves in the outer radiation belt: Cluster STAFF-SA measurements, *J. Geophys. Res. Space Physics*, *118*, 3407–3420, doi:10.1002/jgra.50312.

Albert, J. M. (2005), Evaluation of quasi-linear diffusion coefficients for whistler mode waves in a plasma with arbitrary density ratio, *J. Geophys. Res.*, *110*, A03218, doi:10.1029/2004JA010844.

Albert, J. M., and Y. Y. Shprits (2009), Estimates of lifetimes against pitch angle diffusion, *J. Atmos. Sol. Terr. Phys.*, *71*, 1647–1652, doi:10.1016/j.jastp.2008.07.004.

Benck, S., L. Mazzino, M. Cyamukungu, M. J. Cabrera, and V. Pierrard (2010), Low altitude energetic electron lifetimes after enhanced magnetic activity as deduced from SAC-C and DEMETER data, *Ann. Geophys.*, *28*, 849–859, doi:10.5194/angeo-28-849-2010.

Bortnik, J., R. M. Thorne, and N. P. Meredith (2008), The unexpected origin of plasmaspheric hiss from discrete chorus emissions, *Nature*, *452*, 62–66, doi:10.1038/nature06741.

Chen, L., J. Bortnik, W. Li, R. M. Thorne, and R. B. Horne (2012a), Modeling the properties of plasmaspheric hiss: 1. Dependence on chorus wave emission, *J. Geophys. Res.*, *117*, A05201, doi:10.1029/2011JA017201.

Chen, L., J. Bortnik, W. Li, R. M. Thorne, and R. B. Horne (2012b), Modeling the properties of plasmaspheric hiss: 2. Dependence on the plasma density distribution, *J. Geophys. Res.*, *117*, A05202, doi:10.1029/2011JA017202.

Chen, L., W. Li, J. Bortnik, and R. M. Thorne (2012c), Amplification of whistler-mode hiss inside the plasmasphere, *Geophys. Res. Lett.*, *39*, L08111, doi:10.1029/2012GL051488.

Chen, M. W., and M. Schulz (2001a), Simulations of storm time diffuse aurora with plasmasheet electrons in strong pitch angle diffusion, *J. Geophys. Res.*, *106*(A2), 1873–1886, doi:10.1029/2000JA000161.
Chen, M. W., and M. Schulz (2001b), Simulations of diffuse aurora with plasma sheet electrons in pitch angle diffusion less than everywhere strong, *J. Geophys. Res.*, *106*(A12), 28,949–28,966, doi:10.1029/2001JA000138.
Denton, R. E., J. D. Menietti, J. Goldstein, S. L. Young, and R. R. Anderson (2004), Electron density in the magnetosphere, *J. Geophys. Res.*, *109*, A09215, doi:10.1029/2003JA010245.
Denton, R. E., K. Takahashi, I. A. Galkin, P. A. Nsumei, X. Huang, B. W. Reinisch, R. R. Anderson, M. K. Sleeper, and W. J. Hughes (2006), Distribution of density along magnetospheric field lines, *J. Geophys. Res.*, *111*, A04213, doi:10.1029/2005JA011414.
Glauert, S. A., and R. B. Horne (2005), Calculation of pitch angle and energy diffusion coefficients with the PADIE code, *J. Geophys. Res.*, *110*, A04206, doi:10.1029/2004JA010851.
Golden, D. I., M. Spasojevic, W. Li, and Y. Nishimura (2012), Statistical modeling of plasmaspheric hiss amplitude using solar wind measurements and geomagnetic indices, *Geophys. Res. Lett.*, *39*, L06103, doi:10.1029/2012GL051185.
Kennel, C., and F. Engelmann (1966), Velocity space diffusion from weak plasma turbulence in a magnetic field, *Phys. Fluids*, *9*, 2377–2388, doi:10.1063/1.1761629.
Lerche, I. (1968), Quasi-linear theory of resonant diffusion in a magneto-active, *Relativ. Plasma Phys. Fluids*, *11*, 1720–1727, doi:10.1063/1.1692186.
Li, W., et al. (2013), An unusual enhancement of low-frequency plasmaspheric hiss in the outer plasmasphere associated with substorm-injected electrons, *Geophys. Res. Lett.*, *40*, 3798–3803, doi:10.1002/grl.50787.
Li, W., Q. Ma, R. M. Thorne, J. Bortnik, C. A. Kletzing, W. S. Kurth, G. B. Hospodarsky, and Y. Nishimura (2015), Statistical properties of plasmaspheric hiss derived from Van Allen Probes data and their effects on radiation belt electron dynamics, *J. Geophys. Res. Space Physics*, *120*, 3393–3405, doi:10.1002/2015JA021048.
Lichtenberg, A. J., and M. A. Lieberman (1983), *Regular and Stochastic Motion*, Springer, New York.
Lyons, L. R., and R. M. Thorne (1973), Equilibrium structure of radiation belt electrons, *J. Geophys. Res.*, *78*(13), 2142–2149, doi:10.1029/JA078i013p02142.
Lyons, L. R., R. M. Thorne, and C. F. Kennel (1972), Pitch-angle diffusion of radiation belt electrons within the plasmasphere, *J. Geophys. Res.*, *77*(19), 3455–3474, doi:10.1029/JA077i019p03455.
Meredith, N. P., R. B. Horne, R. M. Thorne, D. Summers, and R. R. Anderson (2004), Substorm dependence of plasmaspheric hiss, *J. Geophys. Res.*, *109*, A06209, doi:10.1029/2004JA010387.
Meredith, N. P., R. B. Horne, M. A. Clilverd, D. Horsfall, R. M. Thorne, and R. R. Anderson (2006a), Origins of plasmaspheric hiss, *J. Geophys. Res.*, *111*, A09217, doi:10.1029/2006JA011707.
Meredith, N. P., R. B. Horne, S. A. Glauert, R. M. Thorne, D. Summers, J. M. Albert, and R. R. Anderson (2006b), Energetic outer zone electron loss timescales during low geomagnetic activity, *J. Geophys. Res.*, *111*, A05212, doi:10.1029/2005JA011516.
Meredith, N. P., R. B. Horne, S. A. Glauert, and R. R. Anderson (2007), Slot region electron loss timescales due to plasmaspheric hiss and lightning-generated whistlers, *J. Geophys. Res.*, *112*, A08214, doi:10.1029/2007JA012413.
Mourenas, D., and J.-F. Ripoll (2012), Analytical estimates of quasi-linear diffusion coefficients and electron lifetimes in the inner radiation belt, *J. Geophys. Res.*, *117*, A01204, doi:10.1029/2011JA016985.
Ni, B., R. M. Thorne, N. P. Meredith, Y. Y. Shprits, and R. B. Horne (2011), Diffuse auroral scattering by whistler mode chorus waves: Dependence on wave normal angle distribution, *J. Geophys. Res.*, *116*, A10207, doi:10.1029/2011JA016517.
Orlova, K., M. Spasojevic, and Y. Shprits (2014), Activity-dependent global model of electron loss inside the plasmasphere, *Geophys. Res. Lett.*, *41*, 3744–3751, doi:10.1002/2014GL060100.
Russell, C. T., R. E. Holzer, and E. J. Smith (1969), OGO 3 observations of ELF noise in the magnetosphere: 1. Spatial extent and frequency of occurrence, *J. Geophys. Res.*, *74*(3), 755–777, doi:10.1029/JA074i003p00755.
Schulz, M., and D. J. Boucher Jr. (1982), Orthogonal basis functions for pitch angle diffusion theory, in *Physics of Space Plasmas (1982–4)*, edited by J. Belcher et al., pp. 159–168, Scientific Publishers, Cambridge, Mass.
Schulz, M., and L. J. Lanzerotti (1974), *Particle Diffusion in the Radiation Belts*, *Phys. Chem. Space*, vol. 7, pp. 215, Springer, New York.
Shprits, Y. Y., R. M. Thorne, G. D. Reeves, and R. Friedel (2005), Radial diffusion modeling with empirical lifetimes: Comparison with CRRES observations, *Ann. Geophys.*, *23*, 1467–1471, doi:10.5194/angeo-23-1467-2005.
Shprits, Y. Y., R. M. Thorne, R. Friedel, G. D. Reeves, J. Fennell, D. N. Baker, and S. G. Kanekal (2006a), Outward radial diffusion driven by losses at magnetopause, *J. Geophys. Res.*, *111*, A11214, doi:10.1029/2006JA011657.
Shprits, Y. Y., W. Li, and R. M. Thorne (2006b), Controlling effect of the pitch angle scattering rates near the edge of the loss cone on electron lifetimes, *J. Geophys. Res.*, *111*, A12206, doi:10.1029/2006JA011758.
Shprits, Y. Y., D. A. Subbotin, N. P. Meredith, and S. R. Elkington (2008), Review of modeling of losses and sources of relativistic electrons in the outer radiation belt II: Local acceleration and loss, *J. Atmos. Sol. Terr. Phys.*, *70*, 1694–1713.
Shprits, Y. Y., D. Subbotin, and B. Ni (2009), Evolution of electron fluxes in the outer radiation belt computed with the VERB code, *J. Geophys. Res.*, *114*, A11209, doi:10.1029/2008JA013784.
Sonwalkar, V. S., and U. S. Inan (1989), Lightning as an embryonic source of VLF hiss, *J. Geophys. Res.*, *94*(A6), 6986–6994, doi:10.1029/JA094iA06p06986.
Spasojevic, M., Y. Y. Shprits, and K. Orlova (2015), Global empirical models of plasmaspheric hiss using Van Allen Probes, *J. Geophys. Res. Space Physics*, *120*, 10,370–10,383, doi:10.1002/2015JA021803.
Thorne, R. M., E. J. Smith, R. K. Burton, and R. E. Holzer (1973), Plasmaspheric hiss, *J. Geophys. Res.*, *78*(10), 1581–1596, doi:10.1029/JA078i010p01581.
Thorne, R. M., et al. (2013), Evolution and slow decay of an unusual narrow ring of relativistic electrons near L ~ 3.2 following the September 2012 magnetic storm, *Geophys. Res. Lett.*, *40*, 3507–3511, doi:10.1002/grl.50627.
Thorne, R., S. Church, and D. Gorney (1979), On the origin of plasmaspheric hiss: The importance of wave propagation and the plasmapause, *J. Geophys. Res.*, *84*(A9), 5241–5247, doi:10.1029/JA084iA09p05241.